IEEE Access
Multidisciplinary | Rapid Review | Open Access Journal

Received January 22, 2019, accepted February 8, 2019, date of publication February 18, 2019, date of current version March 5, 2019.

Digital Object Identifier 10.1109/ACCESS.2019.2899127

SVR Based Blind Signal Recovery for Convolutive MIMO Systems With High-Order QAM Signals

CHAO SUN, LING YANG, LI CHEN, AND JILIANG ZHANG, (Member, IEEE)
School of Information Science and Engineering, Lanzhou University, Lanzhou 730000, China

Corresponding author: Ling Yang (lingyang@lzu.edu.cn)

This work was supported by the International Science and Technology Cooperation Program of China under Grant 2017YFE0118900.

ABSTRACT This paper addresses the blind signal recovery for convolutive multiple-input multiple-output systems with high-order quadrature amplitude modulation (QAM) signals. First, a family of batch blind recovery algorithms is proposed. Concretely, they introduce the error function of multimodulus algorithm and the cross-correlation among different equalizer output vectors into the penalty term of the support vector regression (SVR) framework to recover all sources simultaneously. Then, the corresponding dual-mode blind recovery schemes are constructed to further decrease the interference. The new blind formulation through iterative re-weighted least square achieves low complexity optimization. The SVR framework, in essence, determines that the proposals perform better than the conventional methods in terms of data block size, total interference, and symbol error rate. Moreover, the excellent initialization provided by the first mode and the accurate error expression in the second mode ensure that the SVR-based dual-mode schemes work well with the high-order QAM signals. Finally, the efficiency of the proposals over the classical approaches is evaluated by simulations.

INDEX TERMS Convolutive MIMO systems, high-order QAM signals, blind equalization, blind source separation, support vector regression, multimodulus algorithm.

I. INTRODUCTION

During the past decade, blind signal recovery of convolutive multiple input multiple output (MIMO) systems has been widely studied because of its efficient spectrum utilization through multiple antennas and without assignment of extra bandwidth to pilot. Due to multipath effect and multiple antennas, the received signals suffer from both intersymbol interference (ISI) and interchannel interference (ICI) [1], which manifests blind signal recovery as blind equalization and blind source separation, respectively.

Working on symbol rate, a number of blind equalization approaches using higher-order statistics (HOS) implicitly or explicitly have been studied. Bussgang algorithms, such as constant modulus algorithm (CMA) and multimodulus algorithm (MMA), applying HOS implicitly are the simplest ones. Nevertheless, using in MIMO systems alone, they cannot ensure the extraction of all sources [1]. To overcome this problem, several methods based on successive interference cancellation have been proposed [2]–[6]. They separate sources through eliminating the effect of the recovered sources from the observation, and then the modified observation is fed into the subsequent equalizer to retrieve another source. However, performance degradation is observed in these methods owing to inter-stage propagation of estimation errors [7]. Avoiding this defect, numbers of methods that can recover all sources simultaneously have been presented [1], [8]–[17], which are constructed via adding a separation term on the cost function of equalization. Li and Liu [1] put forward an algorithm based on constant modulus criterion and the cumulant of equalizer outputs. Using second-order cross-correlation among different equalizer outputs to distinguish the sources, CMA [8]–[11] and Shalvi and Weinstein algorithm (SWA) [12], [13] have been extended to MIMO systems resulting in CC-CMA and CC-SWA, which are appealing techniques for their computational simplicity. To solve the random phase rotation and reduce the steady-state error of the above two algorithms, cross-correlation and multimodulus algorithm (CC-MMA) has been put forward [14], [15]. As the stability of these algorithms are easily affected by the initialization, step size and environment noise, and sometimes even divergent, recently, their robust versions have been further studied [16], [17]. Specifically, they work as the corresponding normalized version when the consistency rule is met, otherwise they disregard the cross-correlation term and estimate the dispersion

The associate editor coordinating the review of this manuscript and approving it for publication was Wei Xu.

error by a linear function. Actually, all the above online algorithms ordinarily exist multiple local minima and require huge amounts of samples to converge [18], [19].

High-order quadrature amplitude modulation (QAM) inputs are used to achieve high speed data transmission. However, their constellations are denser than the lower-order ones under the same transmit power, which makes them difficult to recover. For such modulations, HOS based equalization algorithm exhibits a relatively high residual interference, since the error is nonzero when the equalized signal matches with the constellation structure. To solve this problem, hybrid [20]–[22] and dual-mode scheme [23]–[26] have been researched. For dual-mode equalization scheme, when the HOS based approach completes initial convergence, the equalizer is driven by another mode, such as constellation matching error (CME) [23] and decision directed algorithm (DDA) [27], to unceasingly reduce the residual error. Generally, the switching mechanism relies on acceptable initialization interference level which lies on the QAM order and the external noise [28]. In addition, these schemes recover high-order QAM signals in the way of online processing.

In general, batch algorithm can efficiently exploit the statistical information of the received signal to converge with small data blocks. Support vector regression (SVR), based on structural risk minimization, is a valid machine learning tool in dealing with small data blocks, which can be optimized to global minimum. In recent years, it has been used for channel equalization in single input single output (SISO) [29]–[32], orthogonal frequency division multiplexing (OFDM) [33], and MIMO systems [34]. Specifically, in [34], SVR framework combined with CMA and radius directed algorithm (RDA) is researched. Since CMA has poor ability to process multilevel signals, these methods can only process low-order signals such as 4-QAM and 16-QAM. In addition, the defect of random phase rotation exists.

To avoid the shortcomings of online algorithm and recover high-order QAM sources at the same time, SVR framework along with MMA(p, 2) and DDA is considered in this paper. First, we present a family of SVR based batch blind signal recovery algorithms. Concretely, the error function of MMA(p, 2) [35], [36] is introduced into the SVR's penalty term, and the cross-correlation among different equalizer output vectors regarded as an error is combined with the SVR framework to restore all sources simultaneously. After that, a family of dual-mode blind recovery schemes are presented to further reduce the residual interference. The cost functions of above approaches are minimized through iterative re-weighted least square (IRWLS). Our proposals correct the random phase rotation and complete convergence with small data blocks. More importantly, SVR based dual-mode schemes show extremely low residual interference and are suitable for recovering high-order QAM signals.

The remainder of this paper is organized as follows. Section II formulates the MIMO systems model. Section III proposes the novel algorithms and dual-mode schemes along with computational complexity analysis. In Section IV, numerical results are presented to illustrate the performance of the proposals. Finally, Section V concludes this paper.

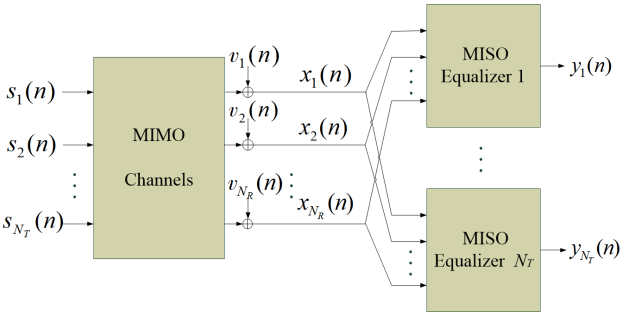

FIGURE 1. Block diagram for MIMO systems blind signal recovery.

II. PROBLEM FORMULATION

The linear time-invariant convolutive MIMO systems depicted in Fig. 1 with N_T transmitters and N_R receivers ($N_R \geq N_T$) are considered. Supposing that the signals of each original source are independently and identically distributed (i.i.d) and each source is independent of others. The original sources $\{s_i(n), 1 \leq i \leq N_T\}$ are propagated to the receivers through different subchannels $\{h_{ij}(n), 1 \leq i \leq N_R, 1 \leq j \leq N_T\}$. $\{x_i(n), 1 \leq i \leq N_R\}$ are received signals disturbed by i.i.d additive white Gaussian noise $\{v_i(n), 1 \leq i \leq N_R\}$. To mitigate ISI and ICI, N_T multiple input single output (MISO) equalizers $\mathbf{w}_i$ ($1 \leq i \leq N_T$) with tap coefficients $\mathbf{w}_i = [\mathbf{w}_{i1}^T, \cdots, \mathbf{w}_{iN_R}^T]^T$ are cascaded. $\{y_i(n), 1 \leq i \leq N_T\}$ are the recovered signals at MISO equalizer i. Given each subchannel $\mathbf{h}_{ij}$ and subequalizer $\mathbf{w}_{ij}$ with length L_h and L_w respectively, the equations linking the above quantities can be expressed as

$$x_i(n) = \sum_j^{N_T} \mathbf{h}_{ij}^T \mathbf{s}_j(n) + v_i(n) \quad i = 1 \cdots N_R, \tag{1}$$

$$y_i(n) = \sum_j^{N_R} \mathbf{w}_{ij}^T \mathbf{x}_j(n) \quad i = 1 \cdots N_T, \tag{2}$$

where $(\cdot)^T$ denotes the transpose operation, $\mathbf{h}_{ij} = [h_{ij}(0), \cdots, h_{ij}(L_h - 1)]^T$ represents the subchannel between transmitter j and receiver i, $\mathbf{s}_j(n) = [s_j(n), \cdots, s_j(n - L_h + 1)]^T$, $\mathbf{w}_{ij} = [w_{ij}(0), \cdots, w_{ij}(L_w - 1)]^T$ is the subequalizer between receiver j and the output of MISO equalizer i, and $\mathbf{x}_j(n) = [x_j(n), \cdots, x_j(n - L_w + 1)]^T$.

Now, the channel input vector $\mathbf{s}(n)$, received signal vector $\overline{\mathbf{x}}(n)$, noise vector $\mathbf{v}(n)$, and channel matrix $\mathbf{H}$ ($N_R \times N_T L_h$) are defined respectively as

$$\mathbf{s}(n) = \begin{pmatrix} \mathbf{s}_1(n) \\ \vdots \\ \mathbf{s}_{N_T}(n) \end{pmatrix}, \overline{\mathbf{x}}(n) = \begin{pmatrix} x_1(n) \\ \vdots \\ x_{N_R}(n) \end{pmatrix}, \mathbf{v}(n) = \begin{pmatrix} v_1(n) \\ \vdots \\ v_{N_R}(n) \end{pmatrix},$$

and

$$\mathbf{H} = \begin{pmatrix} \mathbf{h}_{11}^T & \cdots & \mathbf{h}_{1N_T}^T \\ \vdots & \ddots & \vdots \\ \mathbf{h}_{N_R1}^T & \cdots & \mathbf{h}_{N_RN_T}^T \end{pmatrix}, \tag{3}$$

then (1) can be written in matrix form

$$\bar{\mathbf{x}}(n) = \mathbf{H}\mathbf{s}(n) + \mathbf{v}(n). \tag{4}$$

The equalizer input vector $\mathbf{x}(n)$, equalizer matrix $\mathbf{W}$ ($N_R L_w \times N_T$), and recovered signal vector $\bar{\mathbf{y}}(n)$ are defined respectively as

$$\mathbf{x}(n) = \begin{pmatrix} \mathbf{x}_1(n) \\ \vdots \\ \mathbf{x}_{N_R}(n) \end{pmatrix}, \mathbf{W} = \begin{pmatrix} \mathbf{w}_{11}^T & \cdots & \mathbf{w}_{1N_R}^T \\ \vdots & \ddots & \vdots \\ \mathbf{w}_{N_T 1}^T & \cdots & \mathbf{w}_{N_T N_R}^T \end{pmatrix}^T,$$

and

$$\bar{\mathbf{y}}(n) = \begin{pmatrix} y_1(n) \\ \vdots \\ y_{N_T}(n) \end{pmatrix}, \tag{5}$$

then (2) can be expressed in matrix form

$$\bar{\mathbf{y}}(n) = \mathbf{W}^T \mathbf{x}(n). \tag{6}$$

III. THE PROPOSED METHODS

By introducing the error function of MMA(p, 2) and the cross-correlation among different equalizer output vectors into the SVR's penalty term respectively, we first put forward a family of batch algorithms titled SVR based cross-correlation and multimodulus algorithm SVR-CC-MMA (p, 2). Then, replacing the error of MMA(p, 2) into the error of DDA, SVR based cross-correlation and decision directed algorithm (SVR-CC-DDA) is proposed, and it cascades with SVR-CC-MMA(p, 2) to further reduce residual interference and recover high-order QAM signals. After that, for comparison, DDA is extended to MIMO systems directly resulting in cross-correlation and decision directed algorithm (CC-DDA) which cascades with CC-MMA to construct another dual-mode scheme. Finally, the computational complexity of these algorithms is analyzed.

A. SVR-CC-MMA(p, 2)

In this section, splitting into blind equalization and source separation, the problem of blind signal recovery is formulated. The IRWLS method is utilized for cost function optimization.

Now, the blind equalization problem is considered. We can bring the errors of real and imaginary part respectively into the SVR's penalty term, and then add these two terms together to formulate the final cost function for blind equalization. However, it is found that the computational burden in the process of optimization is relatively high in this way. For the computational simplicity, the blind equalization cost function is deduced as follows. During simulations, we have found that the algorithm using this deduction performs as well as the former.

Assuming that we have gotten N_R observations and each of them is a data block with N symbols, the cost function (3) in [30] is generalized for MIMO systems as

$$F_{BE}(\mathbf{W}) = \sum_{i=1}^{N_T} J_{BE}(\mathbf{w}_i) = \sum_{i=1}^{N_T} \left[\frac{1}{2} \| \mathbf{w}_i \|^2 + C_1 \sum_{n=1}^{N} L_{\varepsilon_1}(u_i(n)) \right], \tag{7}$$

where $J_{BE}(\mathbf{w}_i)$ corresponds to MISO equalizer i, C_1 is the trade-off factor, $u_i(n)$ is the penalty term for the n-th symbol of MISO equalizer i, and $L_\varepsilon(u)$ is usually selected as ε-insensitive loss function

$$L_\varepsilon(u) = \begin{cases} u^2 - 2u\varepsilon + \varepsilon^2, & u \geq \varepsilon \\ 0, & u < \varepsilon, \end{cases} \tag{8}$$

where ε denotes the width of insensitive region.

To link the blind equalization with the SVR framework, we construct $u_i(n) = |e_i(n)|$ with the MMA(p, 2) [35], [36] error function $e_i(n)$ being

$$e_i(n) = \left[\left| |y_{i,R}(n)|^p - R_R^p \right|^2 + \left| |y_{i,I}(n)|^p - R_I^p \right|^2 \right]^{\frac{1}{2}}, \tag{9}$$

where $y_{i,R}(n)$ and $y_{i,I}(n)$ are the real and imaginary part of the n-th symbol in MISO equalizer i, R_R^p and R_I^p containing the prior knowledge about source modulation are defined as

$$R_R^p = \frac{E[|s_{i,R}(n)|^{2p}]}{E[|s_{i,R}(n)|^p]} \text{ and } R_I^p = \frac{E[|s_{i,I}(n)|^{2p}]}{E[|s_{i,I}(n)|^p]}$$

respectively, in which $s_{i,R}(n)$ and $s_{i,I}(n)$ denote the real and imaginary part of $s_i(n)$.

When the function (7) is used alone, multiple MISO equalizers will capture the same source and some of the desired sources are not recovered. Ideally, the equalizer outputs are uncorrelated (cross-correlation value equals 0) when the original sources are i.i.d. Therefore, the cross-correlation among them can regard as an error, which can be used to separate sources blindly. Under the SVR framework, we construct the following cost function

$$\begin{aligned} F_{BSS}(\mathbf{W}) &= \sum_{i=1}^{N_T} J_{BSS}(\mathbf{w}_i) \\ &= \sum_{i=1}^{N_T} \left[\frac{1}{2} \| \mathbf{w}_i \|^2 + C_2 \sum_{j=1; j\neq i}^{N_T} \sum_{\delta=1-\tau}^{\tau-1} L_{\varepsilon_2}(u_{ij}(\delta)) \right], \end{aligned} \tag{10}$$

where C_2 is the trade-off factor, $\tau = L_w + L_h - 1$ is the length of joint impulse response of subchannel and subequalizer, $u_{ij}(\delta) = |c_{ij}(\delta)|$, and $c_{ij}(\delta)$ is the cross-correlation between MISO equalizer i and j with δ delay, defined as

$$c_{ij}(\delta) = \begin{cases} \frac{1}{N} \underline{\mathbf{y}}_i^T \underline{\mathbf{y}}_{j\delta}^*, & \delta \geq 0 \\ \frac{1}{N} \underline{\mathbf{y}}_{i|\delta|}^T \underline{\mathbf{y}}_j^*, & \delta < 0, \end{cases} \tag{11}$$

here $(\cdot)^*$ denotes the conjugate operation, $\underline{\mathbf{y}}_i = [y_i(1), \cdots, y_i(N)]^T$ represents the output vector of MISO equalizer i, $\underline{\mathbf{y}}_{j\delta} = [0, \cdots, 0, y_j(1), \cdots, y_j(N-\delta)]^T$ is gotten via

moving all the elements of $\underline{\mathbf{y}}_j$ down δ units and embedding zero in the front, and $\underline{\mathbf{y}}_{i|\delta|} = [0, \cdots, 0, y_i(1), \cdots, y_i(N-|\delta|)]^T$ is constructed similarly.

To realize blind equalization and source separation simultaneously, function (7) and (10) are added, constructing the final cost function as

$$\begin{aligned} F(\mathbf{W}) &= F_{BE}(\mathbf{W}) + \beta F_{BSS}(\mathbf{W}) \\ &= \sum_{i=1}^{N_T} J_{BE}(\mathbf{w}_i) + \beta J_{BSS}(\mathbf{w}_i) = \sum_{i=1}^{N_T} J(\mathbf{w}_i), \end{aligned} \quad (12)$$

where β is the adjustment factor between source separation and equalization.

The cost function constructed above has no closed form solution, and it is generally minimized by iterative processing. IRWLS with low computational cost than iterative re-weighted quadratic programming (IRWQP) has been successfully applied to the optimization of SVR [37] and proven to converge to the SVR solution [38]. To optimize the cost function (12) and obtain an appropriate recovery matrix $\mathbf{W}$, it is utilized in the next derivation.

After constructing the quadratic approximation of the first order Taylor expansion of $L_\varepsilon(u)$, cost function $F(\mathbf{W})$ can be written as (13), shown at the bottom of this page, where the superscript k represents the number of iterations, $u_i^k(n) = |e_i^k(n)|$ and $e_i^k(n) = [||y_{i,R}^k(n)|^p - R_R^p|^2 + ||y_{i,I}^k(n)|^p - R_I^p|^2]^{\frac{1}{2}}$ is the error with regard to the n-th symbol of MISO equalizer i in the k-th iteration, $u_{ij}^k(\delta) = |c_{ij}^k(\delta)|$ and $c_{ij}^k(\delta)$ is the correlation between MISO equalizer i and j with δ delay in the k-th iteration, CTE is constant terms that do not depend on $\mathbf{W}$, and the weighting factors $a_i(n)$ and $b_{ij}(\delta)$ form as follows

$$\begin{aligned} a_i(n) &= \frac{C_1}{u_i^k(n)} \frac{dL_{\varepsilon_1}(u)}{du}\bigg|_{u_i^k(n)} \\ &= \begin{cases} 0, & u_i^k(n) < \varepsilon_1 \\ \dfrac{2C_1(u_i^k(n) - \varepsilon_1)}{u_i^k(n)}, & u_i^k(n) \geq \varepsilon_1, \end{cases} \end{aligned} \quad (14)$$

$$\begin{aligned} b_{ij}(\delta) &= \frac{C_2}{u_{ij}^k(\delta)} \frac{dL_{\varepsilon_2}(u)}{du}\bigg|_{u_{ij}^k(\delta)} \\ &= \begin{cases} 0, & u_{ij}^k(\delta) < \varepsilon_2 \\ \dfrac{2C_2(u_{ij}^k(\delta) - \varepsilon_2)}{u_{ij}^k(\delta)}, & u_{ij}^k(\delta) \geq \varepsilon_2. \end{cases} \end{aligned} \quad (15)$$

The function $J''(\mathbf{w}_i)$ in (13) is a quadratic approximation to $J(\mathbf{w}_i)$ leading to the same value $J''(\mathbf{w}_i^k) = J(\mathbf{w}_i^k)$ and gradient $\nabla_{\mathbf{w}_i} J''(\mathbf{w}_i^k) = \nabla_{\mathbf{w}_i} J(\mathbf{w}_i^k)$ in the k-th iteration. Therefore, $\mathbf{p}_i^k = \mathbf{w}_i^s - \mathbf{w}_i^k$ can be considered as a descending direction for $J(\mathbf{w}_i)$, where $\mathbf{w}_i^s$ is the least square solution to (13), and it is utilized to construct a linear search approach [39], i.e., $\mathbf{w}_i^{k+1} = \mathbf{w}_i^k + \eta^k \mathbf{p}_i^k$. The value of η^k can be calculated via a backtracking line search [39], and if $J(\mathbf{w}_i^{k+1}) \geq J(\mathbf{w}_i^k)$, it is iteratively declined until a strict decrease in (12) is observed.

$$\begin{aligned} F''(\mathbf{W}) &= \sum_{i=1}^{N_T} J''(\mathbf{w}_i) = \sum_{i=1}^{N_T} J''_{BE}(\mathbf{w}_i) + \beta J''_{BSS}(\mathbf{w}_i) \\ &= \sum_{i=1}^{N_T} \Bigg[\frac{1+\beta}{2} \parallel \mathbf{w}_i \parallel^2 + C_1 \Bigg(\sum_{n=1}^{N} L_{\varepsilon_1}(u_i^k(n)) + \frac{dL_{\varepsilon_1}(u)}{du}\bigg|_{u_i^k(n)} \frac{[u_i(n)]^2 - [u_i^k(n)]^2}{2u_i^k(n)} \Bigg) \\ &\quad + \beta C_2 \Bigg(\sum_{j=1;j\neq i}^{N_T} \sum_{\delta=1-\tau}^{\tau-1} L_{\varepsilon_2}(u_{ij}^k(\delta)) + \frac{dL_{\varepsilon_2}(u)}{du}\bigg|_{u_{ij}^k(\delta)} \frac{[u_{ij}(\delta)]^2 - [u_{ij}^k(\delta)]^2}{2u_{ij}^k(\delta)} \Bigg) \Bigg] \\ &= \sum_{i=1}^{N_T} \Bigg[\frac{1+\beta}{2} \parallel \mathbf{w}_i \parallel^2 + \frac{1}{2} \sum_{n=1}^{N} a_i(n) |e_i(n)|^2 + \frac{\beta}{2} \sum_{j=1;j\neq i}^{N_T} \sum_{\delta=1-\tau}^{\tau-1} b_{ij}(\delta) |c_{ij}(\delta)|^2 \Bigg] + CTE \end{aligned} \quad (13)$$

$$\begin{aligned} \nabla_{\mathbf{w}_i} J''(\mathbf{w}_i) &= (1+\beta)\mathbf{w}_i + p \sum_{i=1}^{N} a_i(n) \\ &\times \Bigg[\Big(|y_{i,R}(n)|^p - R_R^p \Big) |y_{i,R}(n)|^{p-1} \mathrm{sgn}[y_{i,R}(n)] + \jmath \cdot \Big(|y_{i,I}(n)|^p - R_I^p \Big) |y_{i,I}(n)|^{p-1} \mathrm{sgn}[y_{i,I}(n)] \Bigg] \mathbf{x}^*(n) + \beta \mathbf{f} = 0 \end{aligned} \quad (16)$$

$$\begin{aligned} &(1+\beta)\mathbf{w}_i + p \sum_{i=1}^{N} a_i(n) \Big[|y_{i,R}(n)|^{2p-2} y_{i,R}(n) + \jmath \cdot |y_{i,R}(n)|^{2p-2} y_{i,I}(n) \Big] \mathbf{x}^*(n) \\ &= p R_R^p \sum_{i=1}^{N} a_i(n) \Big[|y_{i,R}(n)|^{p-1} \mathrm{sgn}[y_{i,R}(n)] + \jmath \cdot |y_{i,I}(n)|^{p-1} \mathrm{sgn}[y_{i,I}(n)] \Big] \mathbf{x}^*(n) \\ &\quad + \jmath \cdot \sum_{i=1}^{N} a_i(n) \Big[|y_{i,R}(n)|^{2p-2} - |y_{i,I}(n)|^{2p-2} \Big] \times y_{i,I}(n) \mathbf{x}^*(n) - \beta \mathbf{f} \end{aligned} \quad (17)$$

To obtain the least square solution $\mathbf{w}_i^s$ to $J''(\mathbf{w}_i)$, its gradient shown in (16), as shown at the bottom of the previous page, is set to zero, where sgn[·] is the signum function and $\mathbf{f}$ is the derivative of the second term in square bracket of (10) with regard to $\mathbf{w}_i$

$$\mathbf{f} = \frac{1}{N}\sum_{j=1;j\neq i}^{N_T} \times \left[\sum_{\delta=0}^{\tau-1} b_{ij}(\delta)c_{ij}(\delta)\mathbf{X}^H\underline{\mathbf{y}}_{j\delta} + \sum_{\delta=1-\tau}^{-1} b_{ij}(\delta)c_{ij}(\delta)(\mathbf{X}^{(|\delta|)})^H\underline{\mathbf{y}}_j\right],$$

here $(\cdot)^H$ denotes the complex conjugate transpose operation, $\mathbf{X}$ $(N \times N_R L_w)$ and $\mathbf{X}^{(|\delta|)}$ $(N \times N_R L_w)$ represent the MISO equalizer input matrix and its shifting version respectively, writing as

$$\mathbf{X} = \begin{pmatrix} \mathbf{x}^T(1) \\ \vdots \\ \mathbf{x}^T(N) \end{pmatrix} = \begin{pmatrix} \mathbf{x}_1^T(1) & \cdots & \mathbf{x}_{N_R}^T(1) \\ \vdots & \ddots & \vdots \\ \mathbf{x}_1^T(N) & \cdots & \mathbf{x}_{N_R}^T(N) \end{pmatrix},$$

and

$$\mathbf{X}^{(|\delta|)} = \begin{pmatrix} \mathbf{0} & \cdots & \mathbf{0} \\ \vdots & \ddots & \vdots \\ \mathbf{0} & \cdots & \mathbf{0} \\ \mathbf{x}_1^T(1) & \cdots & \mathbf{x}_{N_R}^T(1) \\ \vdots & \ddots & \vdots \\ \mathbf{x}_1^T(N-|\delta|) & \cdots & \mathbf{x}_{N_R}^T(N-|\delta|) \end{pmatrix}.$$

Specifically, $\mathbf{X}^{(|\delta|)}$ is obtained via moving all the vectors of $\mathbf{X}$ down $|\delta|$ units and embedding appropriate zero vector $\mathbf{0}$ on the top.

Using the fact $R_I^p = R_R^p$ for QAM modulation and reordering terms, equation (16) is rewritten as (17), shown at the bottom of the previous page, whose matrix form is

$$[p\mathbf{X}^H\mathbf{D_a}\mathbf{D_b}\mathbf{X} + (1+\beta)\mathbf{I}]\mathbf{w}_i = pR_R^p\mathbf{X}^H\mathbf{D_a}\mathbf{Y_A} + \jmath \cdot p\mathbf{X}^H\mathbf{D_a}\mathbf{Y_B} - \beta\mathbf{f}, \quad (18)$$

where $\mathbf{I}$ is an identity matrix with appropriate size, $\mathbf{D_a}$ and $\mathbf{D_b}$ are diagonal matrices with diagonal elements $a_i(n)$ and $|y_{i,R}(n)|^{2p-2}$ respectively, $\mathbf{Y_A}$ and $\mathbf{Y_B}$ are column vectors containing $|y_{i,R}(n)|^{p-1}\text{sgn}[y_{i,R}(n)] + \jmath\cdot|y_{i,I}(n)|^{p-1}\text{sgn}[y_{i,I}(n)]$ and $(|y_{i,R}(n)|^{2p-2} - |y_{i,I}(n)|^{2p-2})y_{i,I}(n)$ in the i-th row respectively.

The above deduction realizes the IRWLS solution for $J(\mathbf{w}_i)$, which can recover one of the sources. To clearly show the blind recovery of all sources, the SVR-CC-MMA(p, 2) procedure is summarized in **Algorithm 1**.

B. SVR-CC-DDA AND SVR BASED DUAL-MODE SCHEME

In contrast with MMA, the error of DDA is equal to zero for multimodulus signal when the equalizer output coincides with the transmitted signal [28]. Therefore, it possesses the ability to handle high-order QAM signals when the equalizer has been reasonably initialized. As in conventional DDA [27], the error term to be penalized in SVR-CC-DDA is

$$e_i(n) = y_i(n) - \text{dec}[y_i(n)], \quad (19)$$

where dec[·] is the decision function. By the similar derivation as the previous one, the matrix equation to be iterated in the IRWLS method is

$$[\mathbf{X}^H\mathbf{D_a}\mathbf{X} + (1+\beta)\mathbf{I}]\mathbf{w}_i = \mathbf{X}^H\mathbf{D_a}\mathbf{d} - \beta\mathbf{f}, \quad (20)$$

where $\mathbf{d}$ is the column vector that contains dec$[y_i(n)]$ in the n-th row.

The procedure of SVR-CC-DDA is consistent with the SVR-CC-MMA(p, 2), except for

- Step 1: because it works in the second mode of the dual-mode scheme, the initialization matrix $\mathbf{W}^0$ is the value of $\mathbf{W}$ provided by SVR-CC-MMA(p, 2).
- Steps 1, 6 and 10: $e_i(n)$ is computed by (19) rather than (9).
- Step 4: $\mathbf{w}_i^s$ is obtained by solving (20) rather than (18).

In the SVR based dual-mode scheme, first SVR-CC-MMA(p, 2) are used to provide suitable initialization for $\mathbf{W}$, and then SVR-CC-DDA is employed to unceasingly mitigate the residual interference. For simplicity, this process is titled SVR based cross-correlation multimodulus and decision directed scheme SVR-CC-MM(p, 2)-DD.

Algorithm 1 Summary of the SVR-CC-MMA(p, 2) Procedure for Blind Signal Recovery in Convolutive MIMO Systems

1: **initialization**: initialize MIMO equalizer matrix $\mathbf{W}^0 = [\mathbf{w}_1^0, \cdots, \mathbf{w}_{N_T}^0]$, obtain $y_i(n)$ by (2), $e_i(n)$ by (9), $c_{ij}(\delta)$ by (11), calculate $u_i(n) = |e_i(n)|$ and $u_{ij}(\delta) = |c_{ij}(\delta)|$, compute $a_i(n)$ from (14) and $b_{ij}(\delta)$ from (15) ($i, j = 1\cdots N_T$ and $i \neq j$). Set i=1, k=0 and initialize η^0.
2: **repeat**
3: **for** $1 \leq i \leq N_T$ **do**
4: calculate $\mathbf{w}_i^s$ via solving (18).
5: update $\mathbf{w}_i^{k+1} = \mathbf{w}_i^k + \eta^k[\mathbf{w}_i^s - \mathbf{w}_i^k]$.
6: recompute $e_i(n)$, $u_i(n)$, $a_i(n)$, $c_{ij}(\delta)$, $u_{ij}(\delta)$, and $b_{ij}(\delta)$ ($j = 1\cdots N_T$ and $j \neq i$), update $i = i + 1$.
7: **while** $J(\mathbf{w}_i^{k+1}) \geq J(\mathbf{w}_i^k)$ **do**
8: compute $\eta^k = \rho\eta^k$ with $0 < \rho < 1$.
9: update $\mathbf{w}_i^{k+1} = \mathbf{w}_i^k + \eta^k[\mathbf{w}_i^s - \mathbf{w}_i^k]$.
10: recompute $e_i(n)$, $u_i(n)$, $a_i(n)$, $c_{ij}(\delta)$, $u_{ij}(\delta)$, and $b_{ij}(\delta)$ ($j = 1\cdots N_T$ and $j \neq i$).
11: **end while**
12: **end for**
13: set i=1 and update $k = k + 1$.
14: **until** convergence.

C. CC-DDA AND TRADITIONAL DUAL-MODE SCHEME

Inspired by CC-CMA [9], we generalize DDA for MIMO scenario with N_T sources as follows

$$F_{DD}(\mathbf{W}) = E\sum_{i=1}^{N_T}\Big[y_i(n) - \mathrm{dec}[y_i(n)]\Big]^2 + \alpha\sum_{i,j=1;i\neq j}^{N_T}\sum_{\delta=1-\tau}^{\tau-1}|r_{ij}(\delta)|^2, \quad (21)$$

where α is the adjustment factor, and $r_{ij}(\delta)$ is the measurement of correlation between MISO equalizer i and j, which are used to separate different sources, defined as

$$r_{ij}(\delta) = E[y_i(n)y_j^*(n-\delta)]. \quad (22)$$

Stochastic gradient descent is applied to minimize the cost function $F_{DD}(\mathbf{W})$ efficiently, leading to the updating equation

$$\mathbf{W}(n+1) = \mathbf{W}(n) - \mu[\Delta_1(n)\cdots\Delta_{N_T}(n)]\mathbf{x}^*(n),$$

where μ denotes step-size and

$$\Delta_i(n) = 2\Big[y_i(n) - \mathrm{dec}[y_i(n)]\Big] + 2\alpha\sum_{j=1;j\neq i}^{N_T}\sum_{\delta=1-\tau}^{\tau-1}\hat{r}_{ij}(\delta)y_j(n-\delta), \quad (23)$$

here $\hat{r}_{ij}(\delta)$ denotes an estimation of $r_{ij}(\delta)$ and is generally obtained by rectangular window sample averaging.

For high-order QAM signals, CC-MMA exists a relatively high steady-state error, therefore CC-DDA follows it to further mitigate the residual error. In the next section, this online dual-mode scheme titled cross-correlation multimodulus and decision directed scheme (CC-MM-DD) is used for contrast.

D. COMPUTATIONAL COMPLEXITY

This part discusses the computational complexity of the proposals and traditional algorithms. The complexity of these algorithms in one iteration is summarized in Table 1, where L_r is the length of rectangular window.

TABLE 1. Computational complexity of different algorithms.

Algorithm	Computational Complexity
CC-MMA	$O((4N_RL_w+\tau(2L_r+5)(N_T-1))N_T)$
CC-DDA ($\alpha=0$)	$O((4N_RL_w+N_R)N_T)$
SVR-CC-MMA(p, 2)	$O((N_R^2L_w^2+(\tau N_T-\tau+N_T+2)N_RL_w)NN_T)$
SVR-CC-DDA ($\beta=0$)	$O((N_R^2L_w^2+2N_RL_w)NN_T)$

For CC-MMA, the complexity of blind equalization is linear with N_R and L_w, and the complexity of blind source separation is linear with τ and L_r. The complexity order of CC-CMA and CC-DDA ($\alpha \neq 0$) not presented in this table is the same as that of CC-MMA. For the CC-MM-DD, blind source separation can generally be accomplished in the first mode, thus it is appropriate to adopt $\alpha = 0$ in the CC-DDA (i.e., deleting cross-correlation items), which reduces the complexity. For SVR based algorithms, although the complexity contain term pertaining to $N_R^2L_w^2$, the value of N_RL_w is generally small relative to N, so it will not increase sharply. SVR-CC-DDA with $\beta \neq 0$ has the same complexity order as SVR-CC-MMA(p, 2). Similarly, using $\beta = 0$, its complexity will be significantly reduced. By the way, it is pointed out that the complexity of the proposed algorithms is mainly concentrated on solving $\mathbf{w}_i^s$ in (18) and (20), and the computational complexity of the inverse operation involved in these formulas is not high due to the value of N_RL_w is relatively small.

It is stated here that the above results are the complexity of one iteration. Although they are given in mathematical form, the traditional algorithms are online processing, while the SVR based algorithms are batch processing, so it is not easy to compare the complexity intuitively from Table1. Here we give a qualitative conclusion: applying IRWLS optimization method, the computational complexity of SVR based algorithms is comparable to that of conventional algorithms. In the simulation, we will further elaborate on this conclusion.

IV. NUMERICAL RESULTS

In this section, the blind recovery capability of the proposals is evaluated in contrast with CC-CMA, CC-MMA, and CC-MM-DD. All the experiments were implemented in MATLAB 2014a running on a PC with Intel i5 processor (2.3GHz) and 8G RAM. The evaluation indexes include the total interference (TI), convergence probability, symbol error rate (SER), etc. Containing ISI and ICI, the TI [1], [14] for MISO equalizer i is defined as

$$\mathrm{TI}_i = \frac{\sum_{j,n}|g_{ji}(n)|^2 - \max_{j,n}|g_{ji}(n)|^2}{\max_{j,n}|g_{ji}(n)|^2} = \frac{\sum_{n}|g_{ji}(n)|^2 - \max_{j,n}|g_{ji}(n)|^2}{\max_{j,n}|g_{ji}(n)|^2} + \frac{\sum_{l\neq j,n}|g_{li}(n)|^2}{\max_{j,n}|g_{ji}(n)|^2}, \quad (24)$$

where $\mathbf{g}_{ji}$ is the combined impulse response from transmitter j to MISO equalizer i

$$\mathbf{g}_{ji} = \sum_{q=1}^{N_R}\mathbf{h}_{qj} * \mathbf{w}_{iq}, \quad (25)$$

here * is the convolution operator. The first term of the measure function TI in (24) reflects the residual ISI level in the output signal of the MISO equalizer i, and the second term represents the residual ICI level. Unless otherwise specified, 64-QAM modulation and signal to noise ratio (SNR) of 30 dB have been taken into account. By default, the TI threshold is set to -15 dB, as with this level the equalizer is already possible to switch to the DDA based second mode. We consider that the method is convergent if all sources are successfully recovered while the final TI is lower than the given threshold.

The systems considered in simulations are the 2-input/3-output real channel $\mathbf{H}_1$, 2-input/4-output complex channel $\mathbf{H}_2$ [1], and randomly generated complex channel $\mathbf{H}_3$. In particular, $\mathbf{H}_3$ with $L_h = 3$ is a 2-input/4-output system

TABLE 2. Parameter values of different algorithms for 64-QAM signals.

Algorithm \ Parameter	C_1	C_2	ε_1	ε_2	η^0	ρ	β
SVR-CC-MMA(2,2)	1	1	0	0	0.5	0.7	$N/2$
SVR-CC-MMA(3,2)	1	1	0	0	0.3	0.7	$33*N$
SVR-CC-MMA(4,2)	1	1	0	0	0.2	0.7	$2019*N$
SVR-CC-DDA	1	1	0	0	1	0.7	0

whose tap coefficients are modeled as i.i.d complex Gaussian variables with zero-mean and unit variance. In all cases, the MIMO equalizer $\mathbf{W}$ with $L_w = 9$ is initialized to 1 at the positions (5, 2) and (23, 1), and initialized to 0 at the other positions.

After a comprehensive consideration of the TI level, stability and convergence speed of CC-CMA, CC-MMA, and CC-DDA, the value of adjustment factor α is set to 0.2 and step-size μ with different values has been adopted for each subequalizer. The length of rectangular window L_r is set to 10. For the SVR based methods, the situations of $p = 2, 3$, and 4 are studied. As below, the TI_i difference of two successive IRWLS iterations is taken as the termination condition of **Algorithm 1**.

$$\mathrm{TI}_i(k+1) - \mathrm{TI}_i(k) > -10^{-3} \text{ for all } 1 \le i \le N_T. \quad (26)$$

The parameter C_1 and C_2 have no significant impact on the performance of the algorithm except that too small value (less than 0.01) will increase the TI level. It has been observed that usually not a substantive gain can be observed via using a non-zero insensitive region, when the loss function $L_\varepsilon(u)$ defined in (8) is employed. Simulations have illustrated that product $\rho\eta^k$ controls the optimization process, i.e., a relative large value of $\rho\eta^0$ will cause the algorithm to diverge while a smaller value will rise the IRWLS iterations. Generally, the feasible range of adjustment factor β is relatively wide. With too small value, multiple MISO equalizers may target the same source leading to others neglected, while too large value will intensify divergence. We empirically realize that β with the following value can well compromise equalization and source separation

$$\beta = \frac{N}{2} \cdot \frac{E\left[\left||s_{i,L}(n)|^p - R_L^p\right|^2\right]}{E\left[\left||s_{i,L}(n)|^2 - R_L^2\right|^2\right]}, \quad (27)$$

where $s_{i,L}(n)$ denotes the real or imaginary part of $s_i(n)$. For dual-mode scheme, blind source separation is usually implemented in the first mode, therefore, α and β are set to 0 in the iteration to cut down computation cost when the equalizer works in the second mode. According to the above analysis, the parameters in Table 2 are considered to recover 64-QAM signals. In the following, four groups of experiments are designed from different aspects. Except for specific statements, the results are averaged over 500 independent Monte Carlo runs in all evaluations.

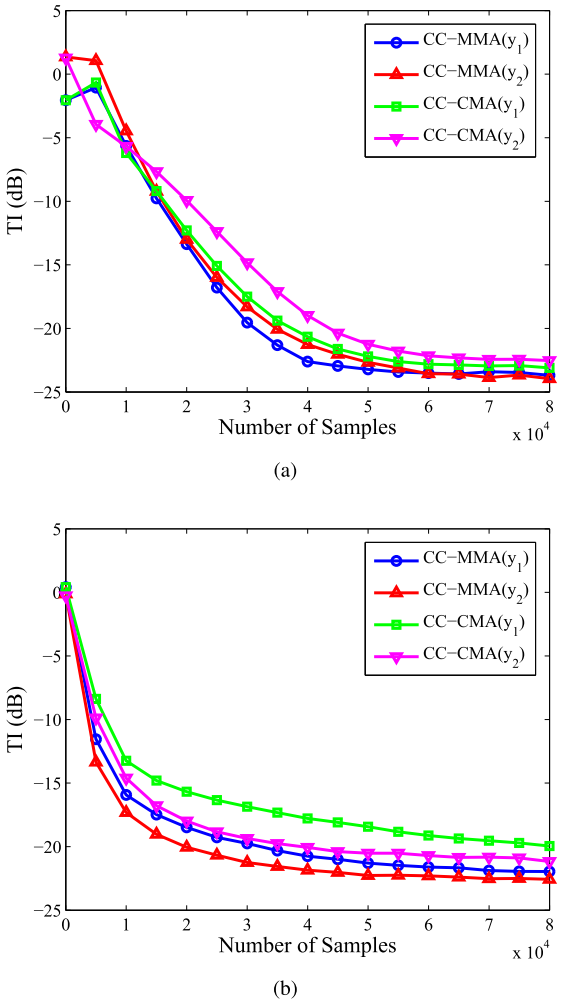

FIGURE 2. TI versus the number of samples for the CC-MMA and CC-CMA. (a) $\mathbf{H}_1$. (b) $\mathbf{H}_1$.

A. SVR-CC-MMA(p, 2) VERSUS CC-MMA AND CC-CMA IN TI LEVEL

Fig. 2 illustrates the TI level achieved by the CC-MMA and CC-CMA. It can be seen that the performance of CC-MMA is better than that of CC-CMA. However, both of them need a huge volume of samples to converge. Taking CC-MMA as an example, about 60000 samples are needed to converge and the final TI levels are about -24 dB and -22 dB respectively for system $\mathbf{H}_1$ and $\mathbf{H}_2$. Fig. 3 depicts the variation of the TI level with data block size N for SVR-CC-MMA(p, 2). Apparently, SVR-CC-MMA(p, 2) with small data blocks perform a lower TI than CC-MMA and CC-CMA. With different value of p, there are significant differences in the TI level, and SVR-CC-MMA(4, 2) shows the best performance. Due to the nonlinear structure of MMA(p, 2) error function, it is difficult to explain why the performance is better when p equals 4. Consistent with [35], we can intuitively explain that the SVR-CC-MMA(p, 2) with a higher dispersion constant (e.g, a larger p) is capable of performing better. However, when p is larger than 4, the appropriate value of η^0 is difficult to select leading to poor robustness.

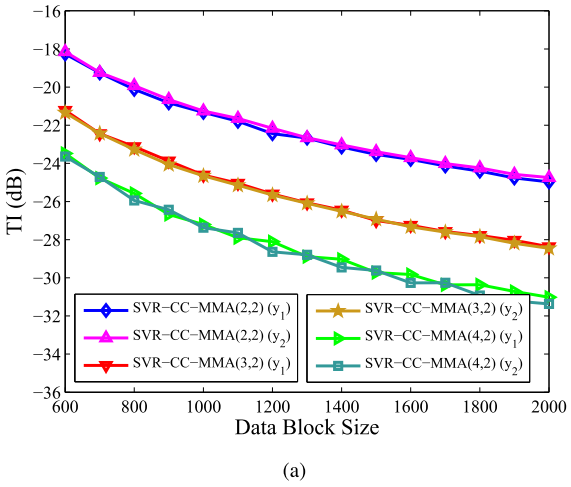

FIGURE 3. TI versus data block size for the SVR-CC-MMA(p, 2). (a) $\mathbf{H}_1$. (b) $\mathbf{H}_2$.

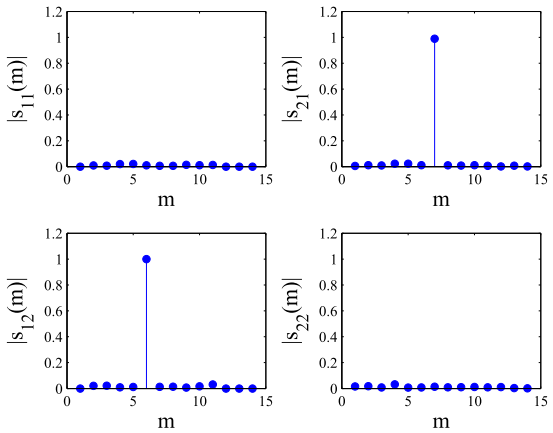

FIGURE 4. The combined impulse responses using the SVR-CC-MMA(2, 2).

With a view to visualize the source separation ability of the SVR-CC-MMA(p, 2), Fig. 4 shows a random implementation of the combined impulse response $\mathbf{g}_{ji}$ when the SVR-CC-MMA(2, 2) is applied to $\mathbf{H}_2$ with $N = 1500$. As we can see that the equalizers compensate the convolution distortion of the channel to a certain extent and capture different sources respectively. Due to the inherent fuzziness in blind signal recovery, MISO equalizer 1 captures source 2 and MISO equalizer 2 captures source 1.

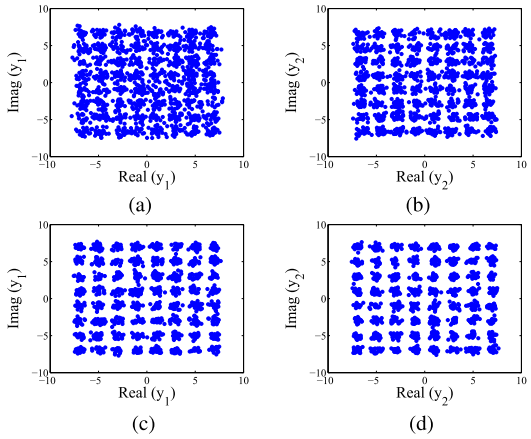

FIGURE 5. Recovered test symbol constellations using single algorithms. (a) CC-MMA. (b) CC-MMA. (c) SVR-CC-MMA(4, 2). (d) SVR-CC-MMA(4, 2).

Fig.5 shows a random implementation of the constellations with 1500 recovered test symbols for $\mathbf{H}_2$. For CC-MMA, the equalizer is trained with 60000 samples, and for SVR-CC-MMA (4, 2), the equalizer is trained with $N = 1500$. It directly exhibits that the equalizer outputs of SVR-CC-MMA (4, 2) are compact than that of CC-MMA. The random phase rotation is corrected, because the cost function is minimized separately in the real and imaginary parts of the signal. Although SVR-CC-MMA (4, 2) represents the best TI level of the family, its constellations are still relatively vague for 64-QAM signals owing to the ambient noise and a higher residual TI. Incidentally, SVR-CC-MMA (p, 2) possess the outstanding ability to blindly recover 16-QAM signals regardless of the value of p.

B. SVR-CC-MM(p, 2)-DD VERSUS CC-MM-DD IN TI LEVEL

In this experiment, the blind signal recovery capability of dual-mode schemes is verified via $\mathbf{H}_2$. Since CC-MMA achieves steady convergence after 60000 iterations, the dual-mode scheme CC-MM-DD is switched to CC-DDA from here. Fig. 6 depicts the convergence process of the TI level with the number of iterations for CC-MM-DD. As shown in it, the TI level has been significantly reduced after switching to CC-DDA. Fig. 7 plots the variation of the TI level with data block size for SVR-CC-MM(p, 2)-DD. Compared with the corresponding single algorithms in Fig. 3b, it is found that SVR-CC-MM(p, 2)-DD can significantly reduce the residual interference of the system. Similar to the decline of CC-MM-DD, the rapid descent process of SVR-CC-MM(2, 2)-DD is shown in Fig. 11, which will be detailedly discussed in group C. Moreover, CC-MM-DD achieves steady-state convergence after 80000 iterations leading to the TI level about -34 dB and -37 dB respectively for equalizer outputs y_1 and y_2, while SVR-CC-MM(p, 2)-DD solely require 700 samples resulting in a lower TI level. Same as the

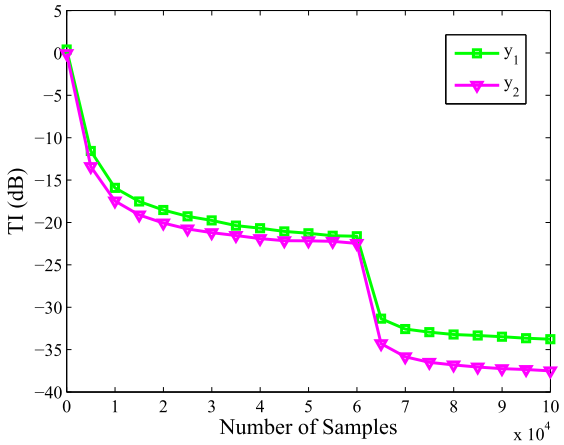

FIGURE 6. TI versus the number of samples for the CC-MM-DD.

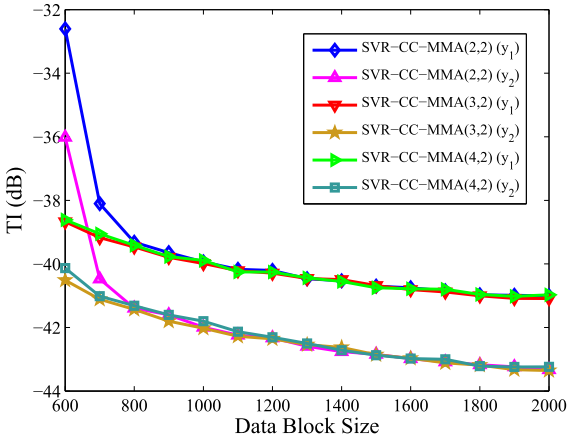

FIGURE 7. TI versus data block size for the SVR-CC-MM(*p*, 2)-DD.

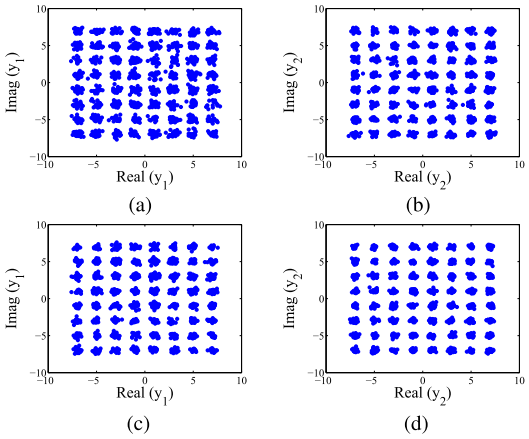

FIGURE 8. Recovered test symbol constellations using dual-mode schemes. (a) CC-MM-DD. (b) CC-MM-DD. (c) SVR-CC-MM(4, 2)-DD. (d) SVR-CC-MM(4, 2)-DD.

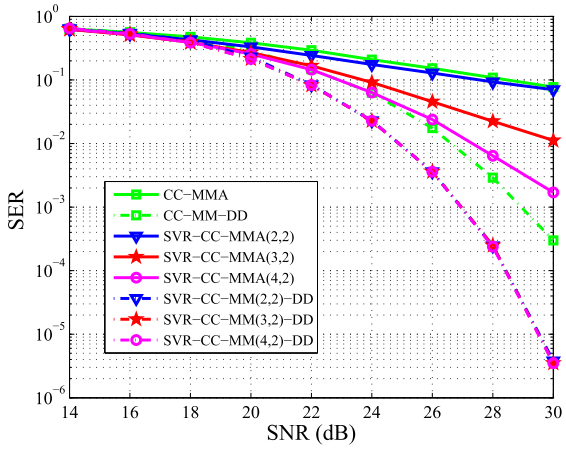

FIGURE 9. SER versus SNR for different methods.

previous experiment, this result again demonstrates the extremely significant advantage of the SVR based methods over the traditional methods in residual TI level and data block size. With the increase of data block size, SVR-CC-MM(p, 2)-DD provide more and more better performance than CC-MM-DD in terms of the TI level. An understandable phenomenon is that once the SVR-CC-MMA(p, 2) provide reliable initialization convergence, the SVR-CC-MM(p, 2)-DD exhibit similar residual TI level regardless the value of p. In Fig. 7, compared with others, SVR-CC-MM(2, 2)-DD exhibits higher residual TI levels in the case of N less than 700, since the data block is too small resulting in the unreliable initial TI level and invalid switching mechanism sometimes.

Under the same parameter settings in Fig. 5, Fig. 8 exhibits the recovered test symbol constellations when CC-MM-DD and SVR-CC-MM(4, 2)-DD are applied. Apparently, the constellations in Fig. 8 are more compact than the corresponding ones in Fig. 5 owing to the fact that the residual TI level is remarkably decreased. For SVR-CC-MM(p, 2)-DD, the clarity of constellation is consistent regardless of the value of p, however, this conclusion is not valid for SVR-CC-MMA(p, 2).

C. THE SIMULATION FOR THE OTHER EVALUATION INDEXES

In this group of experiments, the performance of the proposed algorithms will be simulated from four perspectives: SER, convergence probability, convergence process, and convergence time. The simulation system is $\mathbf{H}_2$.

Figure 9 shows the SER of the whole system over a range of SNR values. For the SVR based methods, equalizer is trained with $N = 1500$. Firstly, under the same SNR, the SER of SVR-CC-MMA(p, 2) are lower than that of CC-MMA, and SVR-CC-MMA(4, 2) owning the lowest SER represents the best performance of single algorithms. Secondly, dual-mode schemes significantly reduce the SER of their corresponding single algorithms under the condition of higher SNR. With the increase of SNR, the noise becomes smaller and smaller while the success rate of mode switching is higher and higher, which make the performance improvement more and more obvious. Finally, we point out that SVR-CC-MM(p, 2)-DD with $p = 2$, 3, and 4 possess the same performance and show the lowest SER.

Fig. 10 indicates that the convergence probability of SVR-CC-MMA(p, 2) vary with data block size. Among

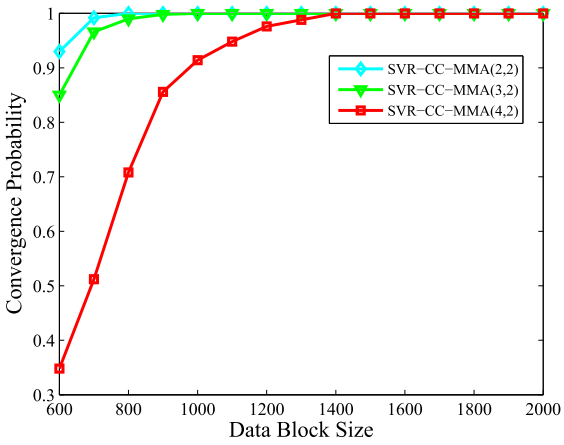

FIGURE 10. Convergence probability versus data block size for the SVR-CC-MMA(p, 2).

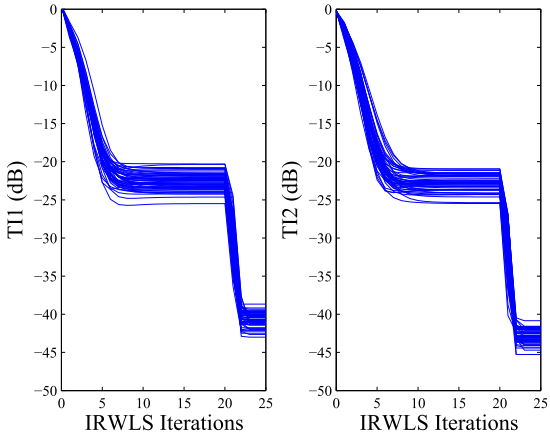

FIGURE 11. TI versus the IRWLS iterations for the SVR-CC-MM(2, 2)-DD in different realizations with $N = 1500$.

them, SVR-CC-MMA(2, 2) providing the best performance can converge all the time when N is more than 700. With the increase of data blocks, the convergence probability of these algorithms is increasing. Dual-mode scheme SVR-CC-MM(p, 2)-DD are constructed by switching to SVR-CC-DDA from the corresponding SVR-CC-MMA(p, 2), thus their convergence probability not presented in the figure is almost the same as the corresponding single algorithms.

With respect to the convergence process of the SVR based methods, Fig. 11 depicts 50 independent realizations of SVR-CC-MM(2, 2)-DD with $N = 1500$. To clearly show the convergence process of each mode, the equalizer switches from SVR-CC-MMA(2, 2) to SVR-CC-DDA after 20 IRWLS iterations. The two subgraphs in Fig. 11 correspond to the convergence process of two MISO equalizers respectively. It can be seen that 10 iterations are enough to achieve convergence for SVR-CC-MMA(2, 2) in all cases while only twice are required for SVR-CC-DDA. Consequently, compared with SVR-CC-MMA(2, 2), dual-mode scheme SVR-CC-MM(2, 2)-DD with slight calculation increment reduces the residual TI level significantly. In the simulation, we have found that the number of iterations required by

TABLE 3. Convergence time (s) of the SVR based algorithms.

Algorithm \ N	1000	1200	1500	1800	2000
SVR-CC-MMA(2,2)	0.98	1.07	1.47	1.90	2.23
SVR-CC-MMA(3,2)	1.43	1.54	1.92	2.45	2.82
SVR-CC-MMA(4,2)	2.57	2.69	3.01	3.64	4.16
SVR-CC-MM(2,2)-DDA	1.21	1.41	1.81	2.29	2.62
SVR-CC-MM(3,2)-DDA	1.61	1.74	2.21	2.79	3.16
SVR-CC-MM(4,2)-DDA	2.76	2.93	3.32	3.90	4.45

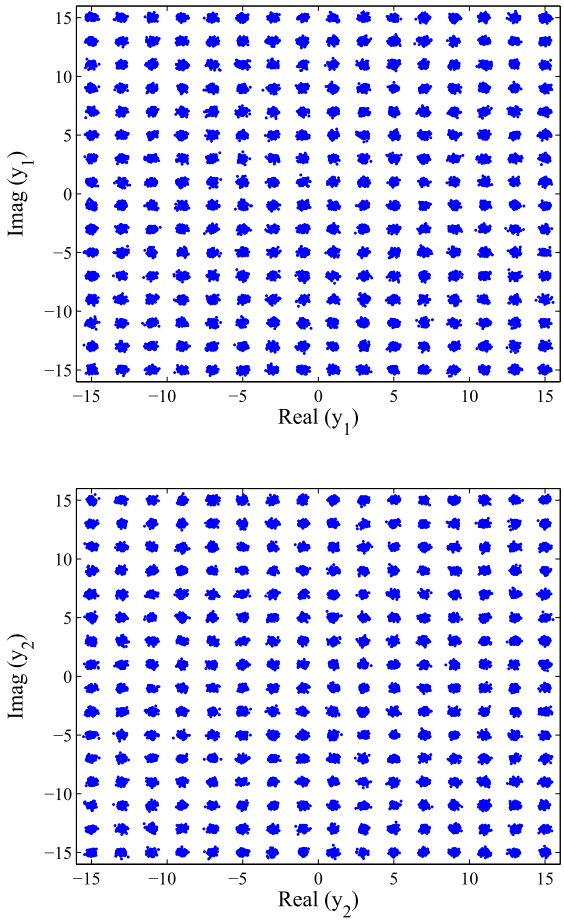

FIGURE 12. Equalizer output constellations of the SVR-CC-MM(4, 2)-DD using 256-QAM with $N = 2000$ and SNR = 35 dB.

different algorithms to achieve convergence is slightly different. In general, SVR-CC-MMA(2, 2) and SVR-CC-DDA perform slightly less iterations than the others. In addition, the number of iterations increases with the decrease of the data block size and the increase of the modulation order.

To further elaborate on computational complexity, the convergence time of different algorithms is counted, although this index is somewhat rough. The convergence times of the CC-CMA, CC-MMA and CC-MM-DD are 2.86s, 2.90s and 3.49s, respectively. The results of the SVR based methods with different data block sizes N are shown in Table 3. All these results roughly illustrate that the proposed algorithms own comparable computational complexity with traditional algorithms. For SVR based methods, under the same data block size, the larger the value of p, the longer the

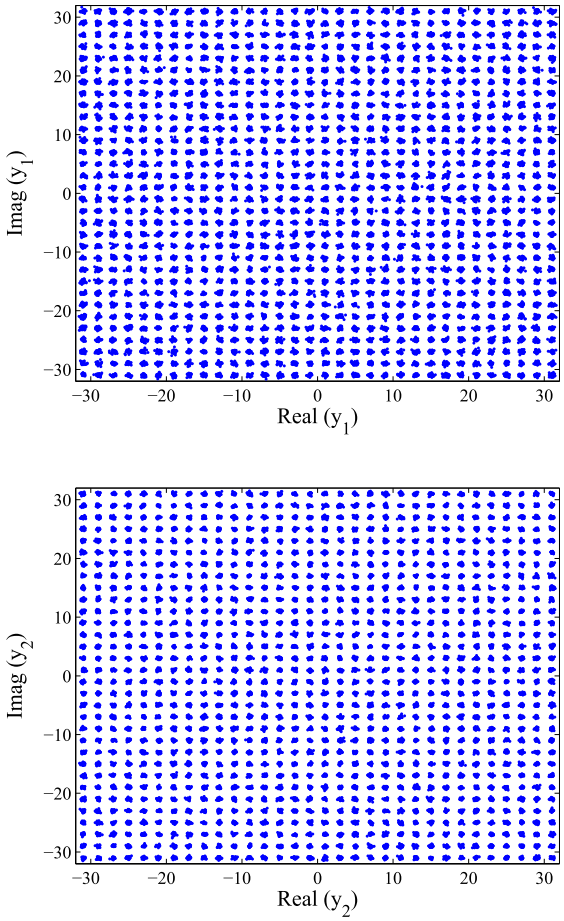

FIGURE 13. Equalizer output constellations of the SVR-CC-MM(4, 2)-DD using 1024-QAM with $N = 3000$ and SNR = 40 dB.

convergence time. The main reason for this phenomenon is that the appropriate η^0 is relatively small at this time, which makes the number of iterations increase. Besides, in dual-mode schemes, the computational cost in the second mode is much less than the first mode. Finally, we point out that the low complexity of the proposals is derived from the IRWLS optimization.

D. DEALING WITH 256-QAM AND 1024-QAM INPUTS

In the last experiment, 256-QAM and 1024-QAM inputs are considered in $\mathbf{H}_3$ under SNR $=$ 35 dB and 40 dB respectively. In the simulation, we have found that CC-MMA cannot provide an acceptable initialization TI under the conditions of these two modulations, which makes the CC-MM-DD always divergent. With the increase of modulation order, SVR-CC-MM(p, 2)-DD require relatively large data blocks (compared to 64-QAM) to achieve signal recovery. In this situation, they possess roughly the same convergence probability whether p is equal to 2, 3, or 4. Since SVR-CC-MMA(4, 2) can provide better initial convergence than the others, thus the corresponding dual-mode scheme SVR-CC-MM(4, 2)-DD is an optimal choice for recovering these two QAM signals. The parameter settings are the same as Table 2 except that β is calculated by (27).

With $N = 2000$, Fig. 12 intuitively shows the recovered 256-QAM constellations with 30000 test symbols. For 1024-QAM modulation, $N = 3000$ are used to train the equalizer and the results with 30000 test symbols are shown in Fig. 13. As shown in these figures, the recovered signals are clear and compact. In addition, a similar recovery effect can be obtained when SVR-CC-MM(4, 2)-DD is applied to $\mathbf{H}_1$ and $\mathbf{H}_2$. However, these results are omitted here since the shortage of space. To the best of our knowledged, the literature does not involve methods that perform similarly to SVR-CC-MM(4, 2)-DD for convolutive MIMO systems with high-order QAM inputs. The results state that it can be applied to blind signal recovery for convolutive MIMO systems with 256-QAM or 1024-QAM inputs.

V. CONCLUSION

We have addressed a family of batch blind signal recovery algorithms from the SVR point of view for linear time-invariant convolutive MIMO systems. Since multimodulus property exists a large nonzero error for high-order QAM inputs when the equalizer outputs match with the constellation, then dual-mode blind signal recovery schemes have been presented to further mitigate residual TI. In contrast with CC-MMA, the novel SVR-CC-MMA(p, 2) with small data blocks achieve a lower residual TI. Dual-mode schemes significantly decrease the SER in higher SNR with respect to single algorithms. Compared with CC-MM-DD, SVR-CC-MM(p, 2)-DD merely use small data blocks to converge and perform a lower residual TI. Consequently, they are applicable to some special scenarios, such as short burst communication. Moreover, the convergence probability, convergence process, and computational complexity are also studied. Finally, we validate the ability of SVR-CC-MM(4, 2)-DD to recover signal for convolutive MIMO systems with 256-QAM and 1024-QAM inputs.

REFERENCES

[1] Y. Li and K. J. R. Liu, "Adaptive blind source separation and equalization for multiple-input/multiple-output systems," *IEEE Trans. Inf. Theory*, vol. 44, no. 7, pp. 2864–2876, Nov. 1998.
[2] J. K. Tugnait, "Blind spatio-temporal equalization and impulse response estimation for MIMO channels using a Godard cost function," *IEEE Trans. Signal Process.*, vol. 45, no. 1, pp. 268–271, Jan. 1997.
[3] H. Furukawa, Y. Kamio, and H. Sasaoka, "Cochannel interference reduction and path-diversity reception technique using CMA adaptive array antenna in digital land mobile communications," *IEEE Trans. Veh. Technol.*, vol. 50, no. 2, pp. 605–616, Mar. 2001.
[4] F. Moazzami and A. Cole-Rhodes, "An adaptive blind equalizer with signal separation for a MIMO system transmitting QAM signals," in *Proc. IEEE Mil. Commun. Conf.*, Nov. 2008, pp. 1–5.
[5] P. O. Taiwo and A. Cole-Rhodes, "MIMO equalization of 16-QAM signal blocks using an FFT-based alphabet-matched CMA," in *Proc. 51st Annu. Conf. Inf. Sci. Syst.*, Mar. 2017, pp. 1–6.
[6] Y. Sun, F. Wang, D. Li, and Z. liu, "MIMO blind equalization algorithm based on successive interference cancellation," *Telecommun. Syst.*, vol. 68, no. 2, pp. 145–150, Jun. 2018.
[7] N. Gu, Z. Guan, S. Nahavandi, and Y. Xiang, "A new blind signal separation algorithm for instantaneous MIMO system," in *Proc. IEEE Globecom*, Nov./Dec. 2006, pp. 1–5.
[8] C. B. Papadias and A. Paulraj, "A space-time constant modulus algorithm for SDMA systems," in *Proc. Veh. Technol. Conf.*, Apr./May 1996, pp. 86–90.

[9] C. B. Papadias and A. J. Paulraj, "A constant modulus algorithm for multiuser signal separation in presence of delay spread using antenna arrays," *IEEE Signal Process. Lett.*, vol. 4, no. 6, pp. 178–181, Jun. 1997.
[10] Y. Luo and J. A. Chambers, "Steady-state mean-square error analysis of the cross-correlation and constant modulus algorithm in a MIMO convolutive system," *IEE Proc.-Vis., Image Signal Process.*, vol. 149, no. 4, pp. 196–203, Aug. 2002.
[11] A. Ikhlef, K. Abed-Meraim, and D. L. Guennec, "Blind signal separation and equalization with controlled delay for MIMO convolutive systems," *Signal Process.*, vol. 90, no. 9, pp. 2655–2666, Sep. 2010.
[12] M. T. M. Silva, M. D. Miranda, and A. N. Licciardi, Jr., "A robust algorithm for blind space-time equalization," in *Proc. IEEE Int. Conf. Acoust., Speech, Signal Process.*, May 2004, pp. 857–860.
[13] M. T. M. Silva and M. D. Miranda, "Tracking analysis of some space-time blind equalization algorithms," in *Proc. 13th Workshop Statist. Signal Process.*, Jul. 2005, pp. 167–172.
[14] Z. H. Lee and W. G. Lim, "Multi-user multimodulus algorithm in blind source separation and equalization for MIMO systems," in *Proc. IEEE 9th Malaysia Int. Conf. Commun.*, Dec. 2009, pp. 234–237.
[15] A. Ikhlef and D. L. Guennec, "A simplified constant modulus algorithm for blind recovery of MIMO QAM and PSK signals: A criterion with convergence analysis," *EURASIP J. Wireless Commun. Netw.*, vol. 2007, no. 15, Oct. 2007.
[16] F. R. M. Pavan, M. T. M. Silva, and M. D. Miranda, "Avoiding divergence in the constant modulus algorithm for blind equalization of MIMO systems," in *Proc. IEEE Sensor Array Multichannel Signal Process. Workshop*, Jul. 2016, pp. 1–5.
[17] F. R. M. Pavan, M. T. M. Silva, and M. D. Miranda, "A numerically robust blind equalization scheme applied to MIMO communication systems," *J. Franklin Inst.*, vol. 355, no. 1, pp. 596–624, Jan. 2018.
[18] B.-J. Kim and D. C. Cox, "Blind equalization for short burst wireless communications," *IEEE Trans. Veh. Technol.*, vol. 49, no. 4, pp. 1235–1247, Jul. 2000.
[19] H.-D. Han, Z. Ding, and M. Zia, "A convex relaxation approach to higher-order statistical approaches to signal recovery," *IEEE Trans. Veh. Technol.*, vol. 66, no. 1, pp. 188–201, Jan. 2017.
[20] A. Benveniste and M. Goursat, "Blind equalizers," *IEEE Trans. Commun.*, vol. 32, no. 8, pp. 871–883, Aug. 1984.
[21] A. Labed, A. Aissa-El-Bey, T. Chonavel, and A. Belouchrani, "New hybrid adaptive blind equalization algorithms for QAM signals," in *Proc. IEEE Int. Conf. Acoust., Speech Signal Process.*, Apr. 2009, pp. 2809–2812.
[22] W. Rao, C. Lu, Y. Liu, and J. Zhang, "Low-complexity hybrid adaptive blind equalization algorithm for high-order QAM signals," *KSII Trans. Int. Inf. Syst.*, vol. 10, no. 8, pp. 3772–3790, Aug. 2016.
[23] S. Barbarossa and A. Scaglione, "Blind equalization using cost function matched to the signal constellation," in *Proc. Conf. Rec. 31st Asilomar Conf. Signals, Syst. Comput.*, vol. 1, Nov. 1997, pp. 550–554.
[24] L. He and M. Amin, "A dual-mode technique for improved blind equalization for QAM signals," *IEEE Signal Process. Lett.*, vol. 10, no. 2, pp. 29–31, Feb. 2003.
[25] C.-P. Fan, C.-H. Fang, H.-J. Hu, and W.-N. Hsu, "Design and analyses of a fast feed-forward blind equalizer with two-stage generalized multilevel modulus and soft decision-directed scheme for high-order QAM cable downstream receivers," *IEEE Trans. Consum. Electron.*, vol. 56, no. 4, pp. 2132–2140, Nov. 2010.
[26] M. T. M. Silva and J. Arenas-Garcia, "A soft-switching blind equalization scheme via convex combination of adaptive filters," *IEEE Trans. Signal Process.*, vol. 61, no. 5, pp. 1171–1182, Mar. 2013.
[27] R. W. Lucky, "Techniques for adaptive equalization of digital communication systems," *Bell Syst. Tech. J.*, vol. 45, no. 2, pp. 255–286, Feb. 1966.
[28] J. M. Filho, M. D. Miranda, and M. T. M. Silva, "A regional multimodulus algorithm for blind equalization of QAM signals: Introduction and steady-state analysis," *Signal Process.*, vol. 92, no. 11, pp. 2643–2656, Nov. 2012.
[29] I. Santamaria, C. Pantaleon, L. Vielva, and J. Ibanez, "Blind equalization of constant modulus signals using support vector machines," *IEEE Trans. Signal Process.*, vol. 52, no. 6, pp. 1773–1782, Jun. 2004.
[30] M. Lázaro, I. Santamaría, J. Vía, D. Erdogmus, "Blind equalization of multilevel signals using support vector machines," in *Proc. 12th Eur. Signal Process. Conf.*, Sep. 2004, pp. 41–44.
[31] M. Lázaro and J. González-Olasola, "Blind equalization using the IRWLS formulation of the support vector machine," *Signal Process.*, vol. 89, no. 7, pp. 1436–1445, Jul. 2009.
[32] X. Ruan *et al.*, "Blind sequence detection using reservoir computing," *Digit. Signal Process.*, vol. 62, pp. 81–90, Mar. 2017.
[33] S. Mhatli, H. Mrabet, I. Dayoub, and E. Giacoumidis, "A novel support vector machine robust model based electrical equaliser for coherent optical orthogonal frequency division multiplexing systems," *IET Commun.*, vol. 11, no. 7, pp. 1091–1096, May 2017.
[34] C. Sun *et al.*, "Blind source separation and equalization based on support vector regression for MIMO systems," *IEICE Trans. Commun.*, vol. 101, no. 3, pp. 698–708, 2018.
[35] S. Abrar and A. K. Nandi, "Blind equalization of square-QAM signals: A multimodulus approach," *IEEE Trans. Commun.*, vol. 58, no. 6, pp. 1674–1685, Jun. 2010.
[36] A. W. Azim, S. Abrar, A. Zerguine, and K. N. Asoke, "Performance analysis of a family of adaptive blind equalization algorithms for square-QAM," *Digit. Signal Process.*, vol. 48, pp. 163–177, Jan. 2016.
[37] F. Pérez-Cruz, A. Navia-Vázquez, P. L. Alarcón-Diana, and A. Artés-Rodríguez, "An IRWLS procedure for SVR," in *Proc. 10th European Signal Process. Conf.*, Sep. 2000, pp. 1–4.
[38] F. Pérez-Cruz, C. Bousoño-Calzón, and A. Artés-Rodríguez, "Convergence of the IRWLS procedure to the support vector machine solution," *Neural Comput.*, vol. 17, no. 1, pp. 7–18, Jan. 2005.
[39] J. Nocedal and S. Wright, *Numerical Optimization*. Berlin, Germany: Springer, 1999.

CHAO SUN was born in Qingdao, China, in 1992. He received the B.S. degree from Shandong Agricultural University, in 2015, and the M.S. degree from Lanzhou University, in 2018. His research interests include channel equalization, mobile edge computing, and machine learning.

LING YANG was born in Zhangye, China, in 1966. She received the B.S. degree in radio physics and the M.S. degree in communication and information systems from Lanzhou University, Lanzhou, China, in 1989 and 1999, respectively, where she is currently an Associate Professor with the School of Information Science and Engineering. Her research interests include digital communication, software-defined radio, and artificial intelligence.

LI CHEN was born in Qingyang, China, in 1992. She received the B.S. degree from the Lanzhou University of Technology in 2015, and the M.S. degree from Lanzhou University, in 2018. Her research interests include digital signal processing and artificial intelligence.

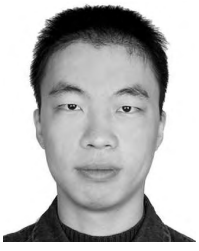

JILIANG ZHANG received the B.S., M.S., and Ph.D. degrees from the Harbin Institute of Technology, in 2007, 2009, and 2014, respectively. He is currently an Associate Professor with the School of Information Science and Engineering, Lanzhou University, China. His research interests include machine learning, MIMO channel measurement and modeling, single radio frequency MIMO system, relay system, and wireless ranging system.